2017

Initial Results of MF-DGNSS R-Mode as an Alternative Position Navigation and Timing Service

Gregory W. Johnson

Peter F. Swaszek
University of Rhode Island, swaszek@uri.edu

Michael Hoppe

Alan Grant

Jan Šafář

Citation/Publisher Attribution

Johnson, Gregory W., Swaszek, Peter F., Hoppe, Michael, Grant, Alan, Safar, Jan, "Initial Results of MF-DGNSS R-Mode as an Alternative Position Navigation and Timing Service," *Proceedings of the 2017 International Technical Meeting of The Institute of Navigation*, Monterey, California, January 2017, pp. 1206-1226.
Available at: https://www.ion.org/ptti/abstracts.cfm?paperID=4696

Initial Results of MF-DGNSS R-Mode as an Alternative Position Navigation and Timing Service

Gregory W. Johnson, Alion Science and Technology
Peter F. Swaszek, University of Rhode Island
Michael Hoppe, German Federal Waterways and Shipping Administration, Germany
Alan Grant and Jan Šafář, General Lighthouse Authorities of the UK and Ireland

BIOGRAPHIES

Gregory W. Johnson is a Senior Program Manager at Alion Science & Technology in the New London, CT office. His group provides research and engineering support primarily to the U.S. Coast Guard R&D Center. Recently he has been working on projects in R-Mode for the German Federal Waterways Administration and AIS for the USCG and the U.S. Army Corps of Engineers. He has a BSEE from the Coast Guard Academy (1987), a MSEE from Northeastern University (1993), and a PhD in Electrical Engineering from the University of Rhode Island (2005). Dr. Johnson has over 20 years of experience in electrical engineering and R&D, focusing on communications, signal processing, and electronic navigation and has published over 85 technical papers. He is a member of the Institute of Navigation, the International Loran Association, the Institute of Electrical and Electronics Engineers, and the Armed Forces Communications Electronics Association. He retired as a Captain in the U.S. Coast Guard Reserves in 2014.

Peter F. Swaszek is a Professor of Electrical Engineering at the University of Rhode Island. His research interests include statistical communication theory, digital signal and image processing, Monte Carlo simulation, and pretty much any problem with an interesting probabilistic/mathematical aspect. His early work focused on data compression and signal detection and estimation in non-Gaussian noise environments. Since a serendipitous sabbatical at the US Coast Guard Academy in 2001, he has been involved in various aspects of electronic navigation including eLoran, DGNSS, and spoofing of GNSS.

Michael Hoppe received his diploma as a radio engineer in 1990. Since 1991 he has been working for the Traffic Technologies Centre within the German Federal Waterways and Shipping Administration. He is responsible for the field of radio navigation systems for maritime and inland waterways applications. Michael Hoppe is a member of various national and international working groups dealing with development and standardization of integrated PNT systems. Since 1998 he has been a member of the IALA Radio navigation committee and since 2006 member of the IALA eNavigation Committee. At present he is acting as vice chair of the PNT WG within the IALA eNavigation Committee.

Dr. Alan Grant is a Principal Development Engineer for the Research and Radionavigation Directorate of the General Lighthouse Authorities of the UK and Ireland, where leads the GNSS and e-Navigation project team. He chairs Working Group 5 of the IALA e-Navigation Committee and is a member of several RTCM special committees. He is a Fellow of the Royal Institute of Navigation and a member of US Institute of Navigation, where he served as maritime representative to Council from 2013 to 2017.

Jan Šafář is an R&D Engineer with the Research and Radionavigation Directorate of the General Lighthouse Authorities of the United Kingdom and Ireland. He holds Masters and PhD degrees in RF engineering from the Czech Technical University, Prague. His areas of expertise include GNSS and complementary technologies for providing resilient positioning, navigation and timing at sea, such as eLoran and enhanced radar positioning. He has been closely involved with the development and international standardisation of the VHF Data Exchange System (VDES) – one of the potential key elements of e-Navigation. He is a member of the Royal Institute of Navigation and the U.S. Institute of Navigation.

ABSTRACT

Position, Navigation, and Timing (PNT) is part of the critical infrastructure necessary for the safety and efficiency of vessel movements, especially in congested areas such as the North Sea. Global Navigation Satellite Systems (GNSS), especially the U.S. Global Positioning System (GPS), have become the primary PNT sources for maritime operations. The GNSS position

is used both for vessel navigation and as the position and timing source for other systems such as Automatic Identification System (AIS).

Unfortunately, GNSS is vulnerable to jamming and interference, intentional or not, which can lead to the loss of positioning information or, even worse, to incorrect positioning information. The user requirement is for dependable PNT information at all times. One potential source of resilient PNT services is Ranging Mode (R-Mode), an alternative PNT concept related to Signals of OPportunity (SoOP) PNT, which uses signals independent of GNSS.

In 2013 the German Federal Waterways and Shipping Administration contracted for a feasibility study of R-Mode using medium frequency (MF) Differential GNSS (DGNSS) and very high frequency (VHF) AIS signals as well as those signals in combination and in combination with eLoran. At ION GNSS+ 2014 some of the authors presented the results from that feasibility study and showed the projected performance using the signals individually and in combination. In most of the shipping lanes on the North Sea it appeared that 10m or better performance could be achieved.

Following up on that work, prototypes of a transmitter and receiver for MF-DGNSS R-Mode have been developed. The transmitter was installed in IJmuiden (Netherlands) and the receiver deployed along the Dutch coast to the south of the transmitter for initial on-air testing of the R-Mode concept; both were synchronized to UTC via GPS. While positioning is not possible with only one R-Mode transmitter, the combination of a synchronized transmitter and receiver pair allows for useful testing of the R-Mode concept. Specifically, the receiver could estimate a true range (rather than a pseudorange); hence, the stability of the range with environmental variations (e.g. weather, day/night skywave effects, etc.) can be studied.

To further study skywave effects, the R-Mode modulator was relocated to a more powerful transmitter at Heligoland (Germany) and the receiver moved to a location near the Kiel Canal (Germany). A second receiver was installed at a similar distance from the transmitter to enable simultaneous comparison of two different propagation paths. Later a third receiver was added in order to provide three paths of different lengths.

The original R-Mode feasibility study also examined the number of stations that it would be possible to receive in the North Sea area to ensure there were sufficient stations for positioning. However, it did not look at the converse question; how would a large number of R-Mode signals impact legacy users. As part of the prototype development, very limited experiments were performed to assess the impact of the new signals on legacy DGNSS receivers. Specifically, during the on-air testing mentioned above, a commercial DGNSS receiver was able to accurately demodulate and decode the on-air transmissions from the single prototype R-Mode transmitter; the impact of multiple signals was not examined. A new study, funded by the General Lighthouse Authorities of the UK and Ireland, has just been initiated to analyze how legacy equipment would respond to multiple R-Mode signals at different frequencies, both in-band and out-of-band.

This paper presents details of the prototype transmitter and receiver and includes statistical analyses of the range estimates recorded to date and the impact of skywave interference at night using data from the German test sites. Additionally, this paper includes preliminary results of the R-Mode signal interference study.

INTRODUCTION

Position, Navigation, and Timing (PNT) is part of the critical infrastructure necessary for the safety and efficiency of vessel movements, especially in congested areas such as the North Sea. Global Navigation Satellite Systems (GNSS), especially the U.S. Global Positioning System (GPS), have become the primary PNT sources for maritime operations. The GNSS position is used both for vessel navigation and as the position and timing source for other bridge systems, such as Automatic Identification System (AIS). Unfortunately, GNSS is vulnerable to jamming and interference, whether intentional or not, which can lead to the loss of positioning information or, even worse, to incorrect positioning information. The user requirement is for dependable PNT information at all times, even under GNSS jamming conditions. A variety of technological solutions to an alternative PNT system are possible; in the radio frequency (RF) domain we have the so-called “Signals of OPportunity” (SoOP) approach (e.g. [1]). This term refers to the opportunistic use of RF signals, typically communications signals, which exist in the geographical area of the receiver. While these signals are not primarily intended for positioning, a SoOP navigation receiver attempts to exploit them as such. Specifically, if each SoOP can provide a (pseudo) range to the receiver from a known location, a trilateration position solution is possible. Usually, there is no alteration of the SoOP signal. In some instances, minor improvements are initiated to improve the signal’s characteristics; for example, synchronizing the signal to a known (and GNSS independent) source of UTC. So called “Ranging Mode” (or R-Mode) is one such example.

In 2013 the German Federal Waterways and Shipping Administration contracted for a feasibility study of R-Mode using medium frequency (MF) differential GNSS (DGNSS) and very high frequency (VHF) AIS signals as well as those signals in combination and in combination with eLoran [2]. This study was part of the European ACCSEAS project. At ION GNSS+ 2014 some of the authors presented the results from that feasibility study and showed the projected performance using the signals individually and in combination [3]. The study stated that the AIS R-Mode was feasible with the existing signal structure (beyond synchronizing the broadcasts and, perhaps, adding a fixed ranging message), but that the DGNSS R-Mode would be greatly improved by actually modifying the signal, adding one or two continuous wave (CW) signals to the broadcast (i.e. not be a pure SoOP, but a hybrid version). In most of the shipping lanes of the North Sea it appeared that 10-meter or better performance could be achieved via R-Mode. Rather than define desired performance up front, the approach of the ACCSEAS project was to try to identify what level of performance was possible and identify what limited the system performance. The decision could then be made as to whether the solution was worth pursuing.

To continue that work, prototypes of an MF-DGNSS R-Mode modulator and receiver were developed; both are reviewed below. The modulator was installed at a transmission site in Ijmuiden (Netherlands) and the receiver deployed to the south along the Dutch coast for initial on-air testing of the R-Mode concept. While positioning is not possible with only one R-Mode transmitter, the combination of a synchronized transmitter and receiver pair allowed for useful testing of the R-Mode concept. Specifically, having both the transmitter and receiver clocks synchronized to a common time source (UTC via GPS in this case, noting that the final full system would be GNSS independent) allows the receiver to estimate a true range (rather than a pseudorange); hence, the stability of the range with environmental variations (e.g. weather, day/night skywave effects, etc.) could be studied. To further study propagation and skywave effects, the R-Mode modulator was relocated to a more powerful transmitter at Heligoland (Germany) in the North Sea and the receiver moved to a location near the Kiel Canal (Germany - east of the transmitter). A second receiver was installed to the west of the transmitter to enable simultaneous comparison of two different propagation paths. A third receiver site, nearly along the signal propagation path to the Kiel Canal, was added most recently. After a brief description of both the modulator and receiver below, experimental results from these receivers are presented.

The R-Mode feasibility study also examined the number of DGNSS transmitters that it would be possible to receive in the North Sea area to ensure there were sufficient stations for positioning [3]. However, it did not look at the related issue; how a large number of R-Mode signals would impact legacy users. As part of the prototype modulator development, very limited experiments were performed to assess the impact of the new signals on legacy DGNSS receivers. Specifically, during all of the on-air testing mentioned above, a commercial DGNSS receiver was able to accurately demodulate and decode the on-air transmissions from the single prototype R-Mode transmitter; however, the impact of multiple signals was not examined. A new study has just been initiated by the General Lighthouse Authorities of the United Kingdom and Ireland to analyze how legacy equipment would respond to multiple R-Mode signals at different frequencies, both in-band and out-of-band. Preliminary results from that work are also reviewed herein.

BACKGROUND ON MF DGNSS BROADCASTS

The MF DGNSS system transmits its information via a binary modulation method known as Minimum Shift Keying (MSK) [4]. Assuming that the MSK transmission is controlled by a precise time/frequency source, both the times of the bit transitions (potentially once every 10 milliseconds) and the underlying phase of the transmitted signal (a sinusoid at approximately 300 kHz) could be exploited to estimate the time of arrival (TOA) for ranging applications. The R-Mode feasibility report examined the potential performance of estimators of time of arrival (TOA) from these two parameters [2]. It was argued that with the existing signal strengths and beacon locations, the time of bit transition is too imprecise for effective ranging. However, assuming that the cycle ambiguity could be resolved, the carrier phase could yield sufficient accuracy. Further, while this level of performance is conceptually possible with the direct MF transmission, it would be significantly easier if in-band continuous wave (CW) signals accompanied the MF and the phase of this separate CW was estimated (similar to Omega [5]). The system proposed in [2] adds two CW signals to the MSK transmission; one below and one above the MSK carrier. Nominal values for the offset in frequency from the MSK carrier are ±225 Hz (recall that the European standards for DGNSS call for a 500 Hz channel bandwidth).

Ranging on the CW signals was analyzed and a bound on estimation accuracy was determined in [2, 6]. For phase estimation the Cramer-Rao lower bound on accuracy is

$$\sigma^2_{\tau\,\widehat{carrier}} \geq \frac{1}{2\omega_c{}^2 T\, SNR}\, seconds$$

in which T is the observation period, ω_c is the MF carrier frequency (in radians per second), and SNR is the received signal to noise ratio. Converting to meters and taking a square root yields the standard deviation

$$\sigma_{MF\ carrier} \geq \frac{1.2\times10^4}{\omega_c\sqrt{T\ SNR}}\ meters$$

Figure 1 shows the potential performance (measured in meters of standard deviation) as a function of signal to noise ratio (SNR) (in dB based upon predicted signal levels and typical North Sea noise values in dBμV). The lines labeled "weak" and "typical" suggest the level of performance available in the North Sea region assuming a 5-second averaging window on the estimator.

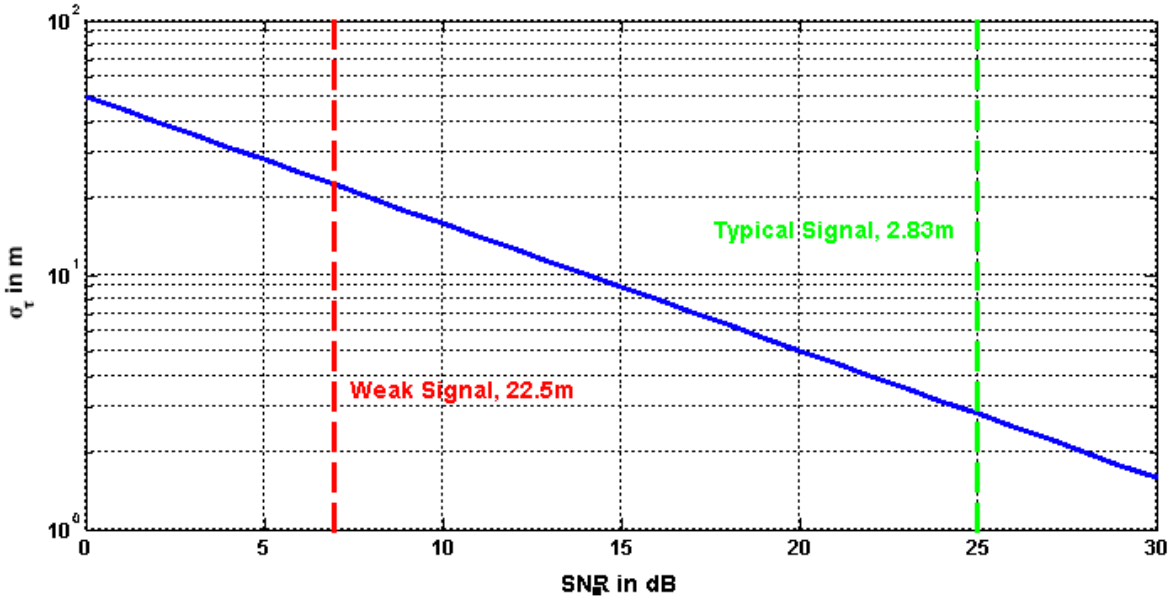

Figure 1: The Cramer-Rao lower bound on performance of estimating the time of arrival from the phase of the MF ranging signal as a function of signal to noise ratio.

There are several important points to remember for MF DGNSS ranging:

- Ranging using carrier phase requires the resolution of cycle ambiguity, the fact that the phase repeats every wavelength of the signal (this is approximately 1 km for MF DGNSS signals). CW signals allow for several ambiguity resolution approaches: (1) initializing the receiver at a fixed location and "counting" cycles as the platform moves or (2) using time synchronized, multiple frequency signals and solving for a position that simultaneously satisfies all of the ambiguity equations with integer solutions. Such solutions have been discussed since the introduction of Omega, which also used different frequencies from spatially separated transmitters (e.g. [7]).
- The propagation of an MF transmission is delayed according to the characteristics of the ground over which it is traveling [8, 9]. These so-called Additional Secondary Factors (ASFs) must be taken into account for positioning applications. While computer modelling tools can predict ASFs using databases of ground conductivity and topography, the quality of the prediction is typically insufficient for the desired positioning accuracy; the tools also do not describe the time varying nature of the ASFs. The current solution to ASFs involves surveying the area of interest to account for spatial effects based upon topography and ground conductivity and establishing monitor sites (with appropriate communications links) to provide temporal corrections to account for the time variation in the delay [10].
- Finally, MF transmissions can suffer from multipath interference due to signal reflections off of the ionosphere; this is referred to as skywave interference [11] and the effect is most pronounced at night. While pulsed signals (such as Loran) can mitigate this effect, continuous transmission (as in MF R-Mode) will always suffer from it; the result is limited coverage range for each transmitter.

PROTOTYPE TRANSMITTER

To implement the CW version of DGNSS R-Mode a new modulator/transmitter is necessary:

1) While the legacy DGNSS transmissions have a specification of time stability [12], precise timing of the transmitted signal is key to accuracy in a pseudo-range-based positioning system; hence, a very stable (e.g. rubidium) clock and a UTC time base with 50 nsec synchronization accuracy are required at each transmission site.
2) Both the MSK and CW signals must be created at the transmitter site. This could be accomplished with a new, integrated modulator or the analog combining of low-level RF signals from a legacy MSK modulator and signal generators for the CW signals. In the second approach, the signal generators must be able to use precise clock and UTC synchronization signals in creating the CW.
3) The transmitter (amplifier) must be able to accommodate the resulting non-constant amplitude signal.
4) The antenna/coupler must be able to accommodate the wider bandwidth signal.

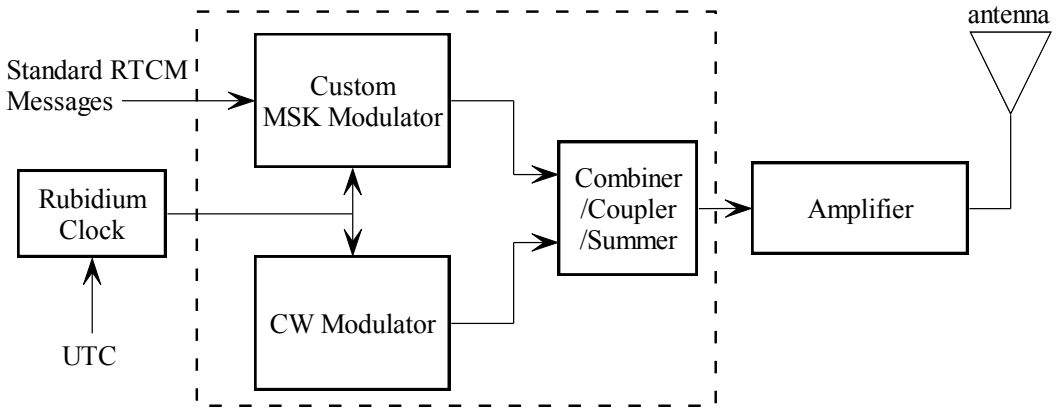

Figure 2: Block diagram for a prototype R-Mode transmitter.

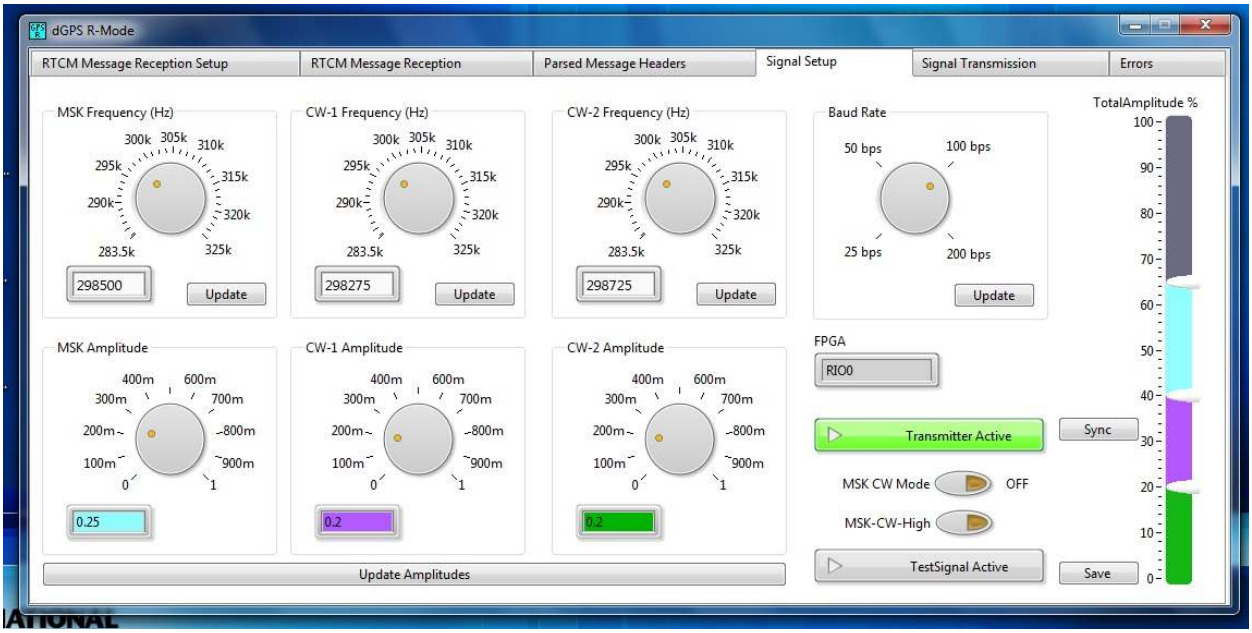

Figure 3: System configuration screen for Novator modulator.

Figure 2 contains a basic block diagram of this modulator/transmitter system. For the testing described in this paper, both routes mentioned in item 2 above were employed to establish R-Mode transmit sites:

- A custom transmitter was constructed by Novator Solutions (Sweden). The unit accepts 10 MHz and 1 pulse per second (PPS) signals for synchronization and allows for adjustment of the relative and absolute power levels in the MSK and CW signals (see Figure 3). It also was designed so that the CW frequencies can be varied in 1 Hz increments.
- The signal was also created using a standard MSK modulator, two high-quality signal generators, and an RF combiner.

PROTOTYPE RECEIVER

In order to study the channel's effects on the MSK and CW signals, a prototype digital R-Mode receiver was developed. Figure 4 contains a basic block diagram of the receiver:

- An analog DGNSS-band front end (filter and amplifier) is used to reduce out-of-band noise and interference due to signals in the adjacent low frequency (LF) and amplitude modulation (AM) bands. While a constant time delay is acceptable as it is removed in a trilateration solution, it is important that this analog front end not introduce *different* time delays for the different DGNSS channels.
- An analog-to-digital converter (ADC) sufficiently fast so as to record the entire DGNSS band as one signal is needed for synchronous signal processing (currently a 1 MHz sampling rate is used). A stable (e.g. rubidium) clock and a UTC time base allow this ADC to precisely collect the MF R-Mode data. While current testing is using only one DGNSS broadcast, future testing will be multi-signal; hence, the collection of the entire DGNSS band.
- A standard MSK demodulator block – this is done in software.
- A CW phase estimator (software block) to estimate the phases of the two transmitted CW signals.

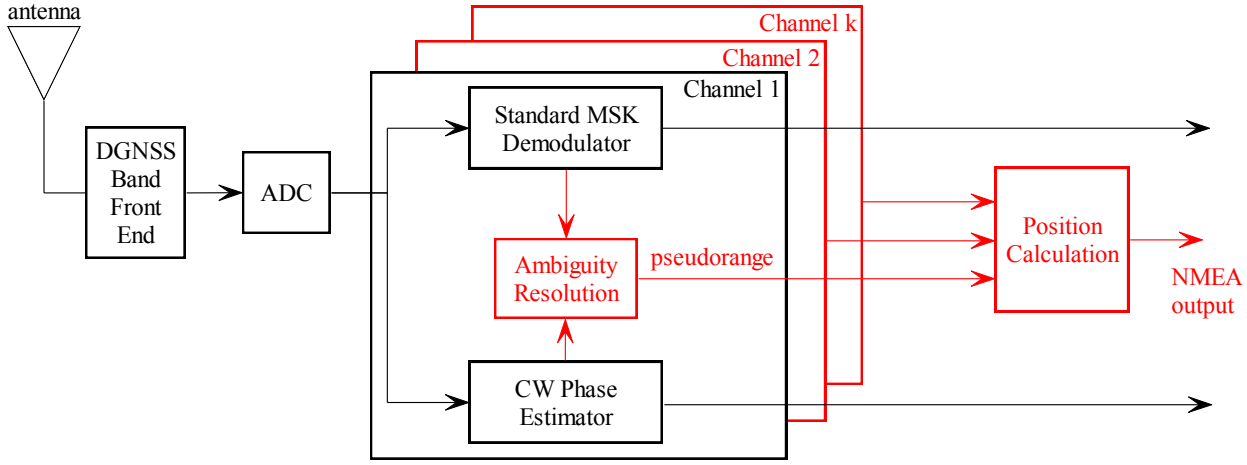

Figure 4: A prototype R-Mode receiver. The portions in red are not yet implemented.

The current prototype receiver demodulates the MSK transmission and estimates the phase angles of the two R-Mode CW signals for a single DGNSS channel; it does not yet attempt this processing for multiple DGNSS channels (although this capability is about to be introduced to the prototype receiver) or resolve the cycle ambiguities, nor does it trilaterate to find the receiver's position (these yet to be added capabilities are shown in red in the figure). Likewise, there are no ASF corrections in the current prototype solution. The algorithm employed is the standard phase estimator for sinusoids in white noise; details on the processing appear in Appendix A. Currently a 5-second block of data is read in and used to estimate the phase. This value was chosen so as to yield moderate phase accuracy (longer data records yield better estimates) while also limiting impacts on accuracy of a moving receiver (any motion over the processing period smears the phase estimate).

ANALYSIS OF TEST DATA

At night MF broadcasts can suffer from multipath interference due to signal reflection off of the ionosphere, so-called skywave; Figure 5(left) shows a simplified view of this reflection. We note:

- The skywave signal appears *later in time* than the ground wave signal (on the order of 100's of μsec later) since the propagation path is longer. Figure 5(right) shows the typical time delays observed versus distance from the transmitter for a one-hop skywave (this is simply based upon the difference in the lengths of the two paths).
- The combination of the direct path plus skywave can cause considerably larger variation in the phase estimate with lower correlation between the two CW frequencies. Theoretically the skywave appears to be another CW signal, of the same frequency, but with different amplitude and phase. Such signals can add constructively or destructively (called fading), and can greatly impact the accuracy of the phase measurement.
- Skywave impacts are larger at further distances from the transmitter since the ground wave experiences higher attenuation than does the skywave; the relative signal powers are measured as a fade margin on a dB scale (ground wave minus skywave power), which can go negative (i.e. the skywave being stronger than the ground wave) [13].

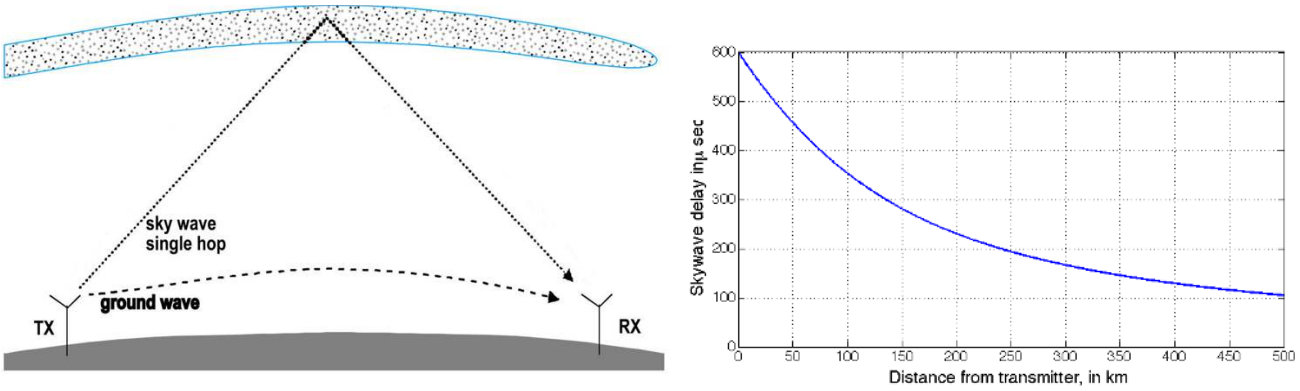

Figure 5: Skywave: left – a simplistic geometrical model; right – the time delay for this model (90 km ionospheric height) versus distance from the transmitter.

Skywave Impact on Ranging

To limit the impacts of noise and skywave on ranging accuracy, it is clear that a short operating range for MF DGNSS R-Mode is preferred; toward this end the ranges for the "shake-down" testing of the prototype transmitter and receiver along the Dutch coast were on the order of 25-50 km. While the density of DGNSS transmitters in the North Sea area is high, trilateration solutions will still require accurate estimation of pseudoranges out to 150 or, perhaps, 200 km. To assess the performance at such typical distances the MF DGNSS R-Mode transmitter was relocated to Heligoland, an archipelago off of the German coast in the North Sea (see Figure 6) and three receiver locations were chosen: Terschelling (213 km from the transmitter), the East end of the Kiel Canal (130 km), and Tönning (66 km).

In the three figures that follow, only data from CW1 is examined as the data from CW2 is virtually identical (it is spaced only 450 Hz away and at the same power).

Figure 7 shows the SNR values over a 4-day period (1-4 Dec 2016) for the CW1 signal as received at each of the three sites. For clarity, the 5-second data samples have been filtered and decimated into data points every 5 minutes. The SNRs for Tönning and the Kiel Canal are similar at night; during the day it appears that there is some local interference source that lowers the SNR by about 3dB at Tönning. The noise source started later on 3 Dec (Saturday) and was not present on the 4th (Sunday). The green lines on this and in the next two figures indicate sunrise and the cyan lines indicate sunset.

Figure 6: Location of the transmitter (red) and three receivers (blue).

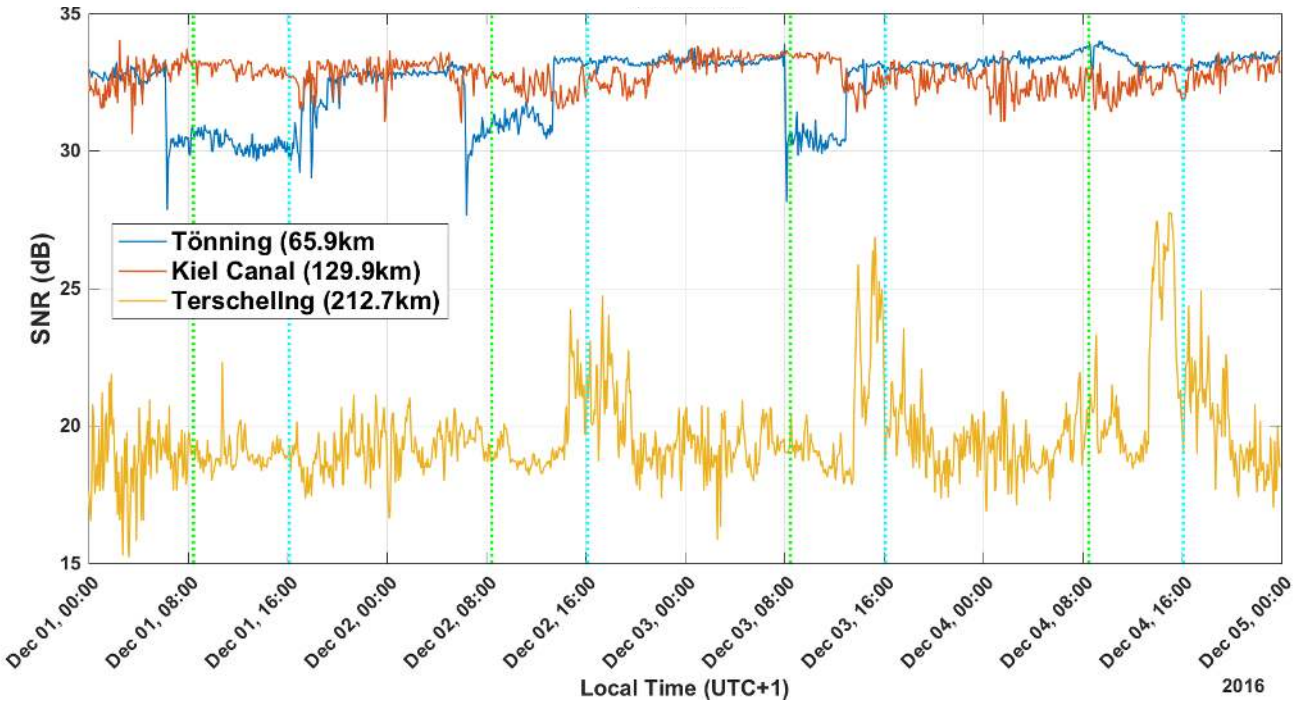

Figure 7: SNR values for CW1 for all three sites, 1-4 Dec.

The stability and quality of the phase measurements can be seen in Figure 8. In this figure, the raw phase measurements have been converted to meters and are shown relative to the mean value. Again the 5-second data samples have been filtered and decimated to 5-minute samples. In order to improve readability, the second and third lines have been offset up from the first (by 50 and 100 meters, respectively). All three receive sites exhibit more noise in the phase measurements during the night

(between the green and cyan lines), which is expected due to the skywave propagation; however, this is much more obvious in the longer signal paths of the Terschelling data. The impact of this increase in noise is quantified in Figure 9, which shows the standard deviations in the phase measurements versus time (note that these are 1-sigma values). Each data point in Figure 9 is the standard deviation of the previous 1-hour of samples (nominally 720 5-second intervals). During the day, the standard deviations are in the 2-3 m range for the two closer sites and 5-10 m for the more distant site. At night due to the impact of skywave, the values increase to 4-10 m for the closest site, and from 10-20 m for the midrange site, and up to 40 m or so for the farthest site. The averages of the standard deviation across all of the day (sunrise to sunset) and night periods are shown in Table 1.

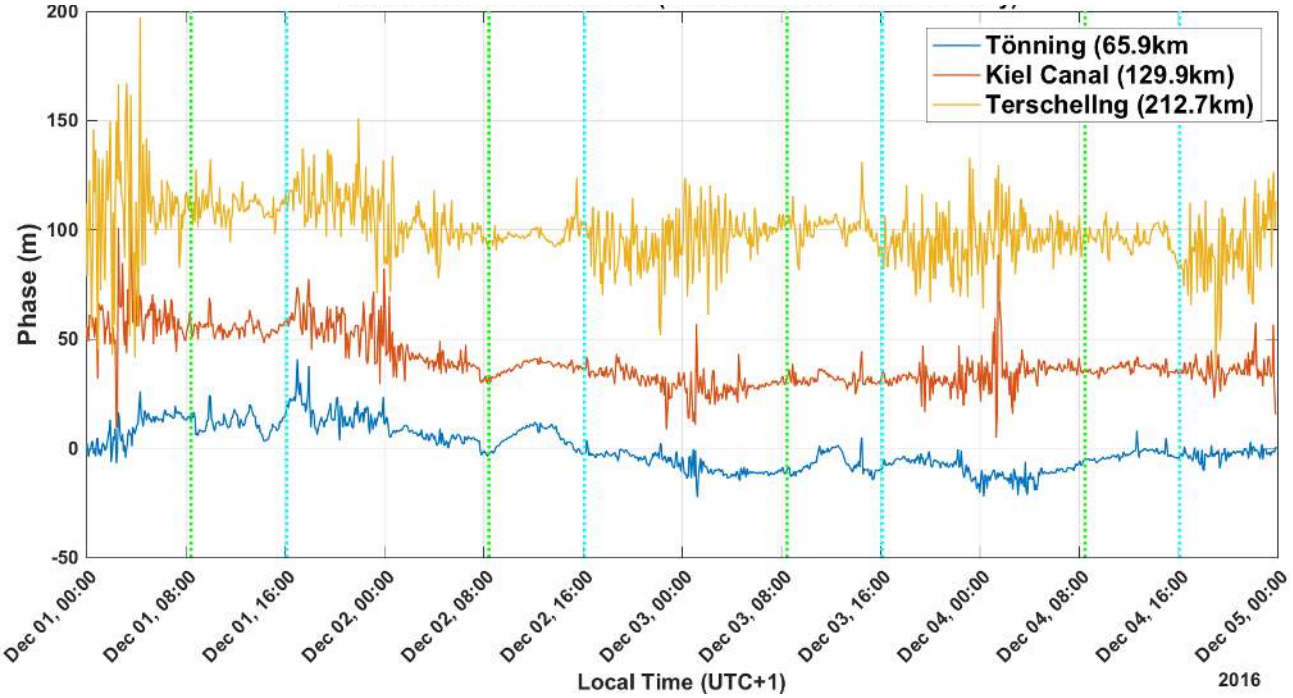

Figure 8: CW1 phase estimates for each site over the period 1-4 Dec. Phase is in meters relative to the mean, with offsets added to Kiel Canal and Terschelling to improve readability of the graphs.

This skywave impact can be seen in the much larger standard deviations at night in Figure 9. These values increase the most at night for the farthest stations (see averages in Table 1). However, in all cases these standard deviations are small enough to allow for trilateration-based positioning. The decrease in SNR did not seem to impact performance appreciably.

In addition to the impact of the skywave, variations in the phase measurement over the course of the day can also be seen. The small scale variations in range experienced during the day (the range values appear to be wandering a bit) are likely due to weather induced fluctuations in the conductivity of the propagation path; similar temporal variation has been observed in 100 kHz Loran signals [10].

Table 1: Average standard deviations for day and night.

	Average Standard Deviation (m)	
Site	**Day**	**Night**
Tönning	2.3	4.3
Kiel Canal	3.1	10.7
Terschelling	7.1	20.5

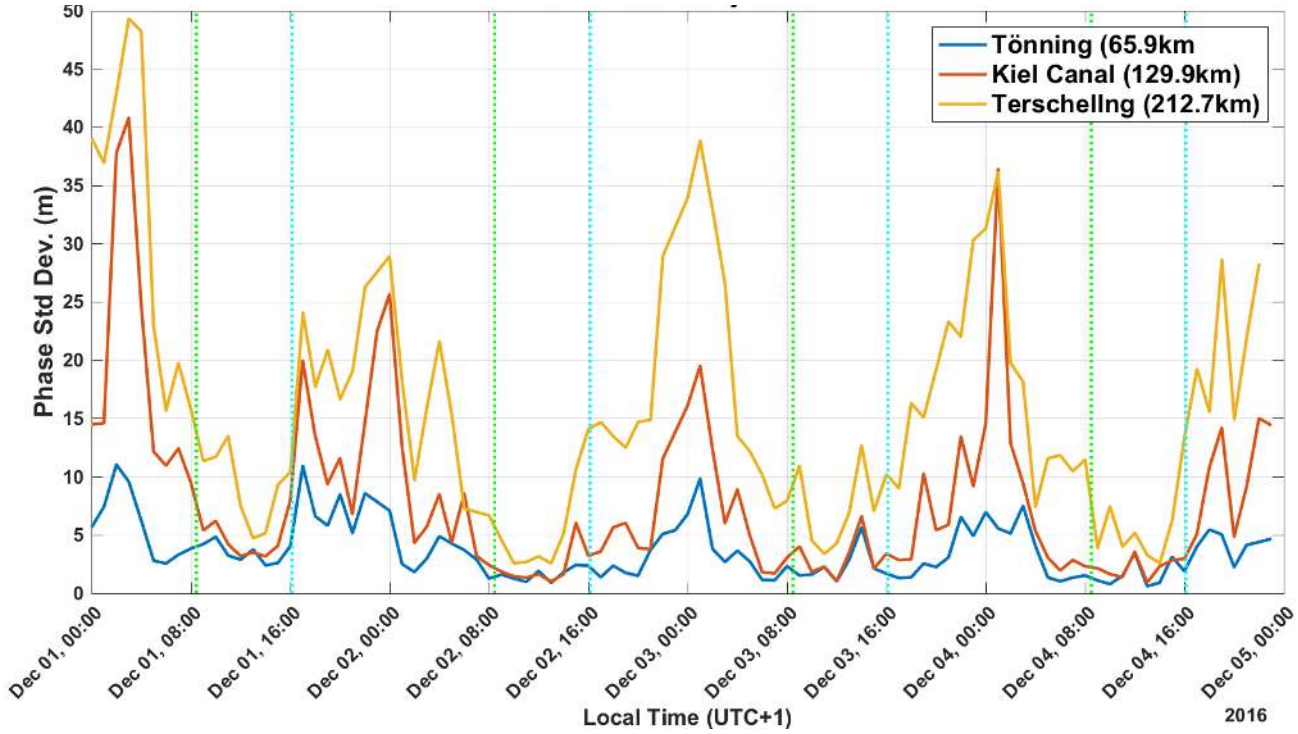

Figure 9: Standard deviation on phase measurements for each of the three receiver sites, 1-4 Dec.

Simulated Positioning Performance

As the R-Mode project develops, it is of interest to assess the positioning performance that would be achieved; unfortunately, positioning is not possible with a single transmitter. However, we can consider the experiment in which we reverse the roles of the transmitter and receivers; specifically, solving for the "unknown" transmitter's location based upon the range measurements and the "known" locations of the three receivers.

The data for this experiment is actual ranges, equal to the measured phase plus an integer number of wavelengths of the CW so that, on average, the range is accurate for the known locations. The solution method is an iterative least squares solution of the range equations (similar to the trilateration solution method for Loran or GPS, but assuming that the clock offset term is zero). Unfortunately, the dilution of precision (DOP) for the actual receiver locations is quite high (>30!) and the solved positions would have a very strong north-south scatter; hence, for this experiment, the "location" of the Kiel Canal site was rotated to be due south of Heligoland, but at the same distance, to improve the geometry and reduce the DOP (see Figure 10).

The performance of such an experiment is shown in Figure 11 using a portion of the range data from Figure 8. The left subfigure shows the error scatter for a 6 hour period during the day; we note the tight scatter and the small 95% (2-sigma) error radius. The right subfigure shows the error scatter for a 6 hour period during the night, during a period with large range variation; although the error scatter has grown, its 95% (2-sigma) error radius is still quite reasonable.

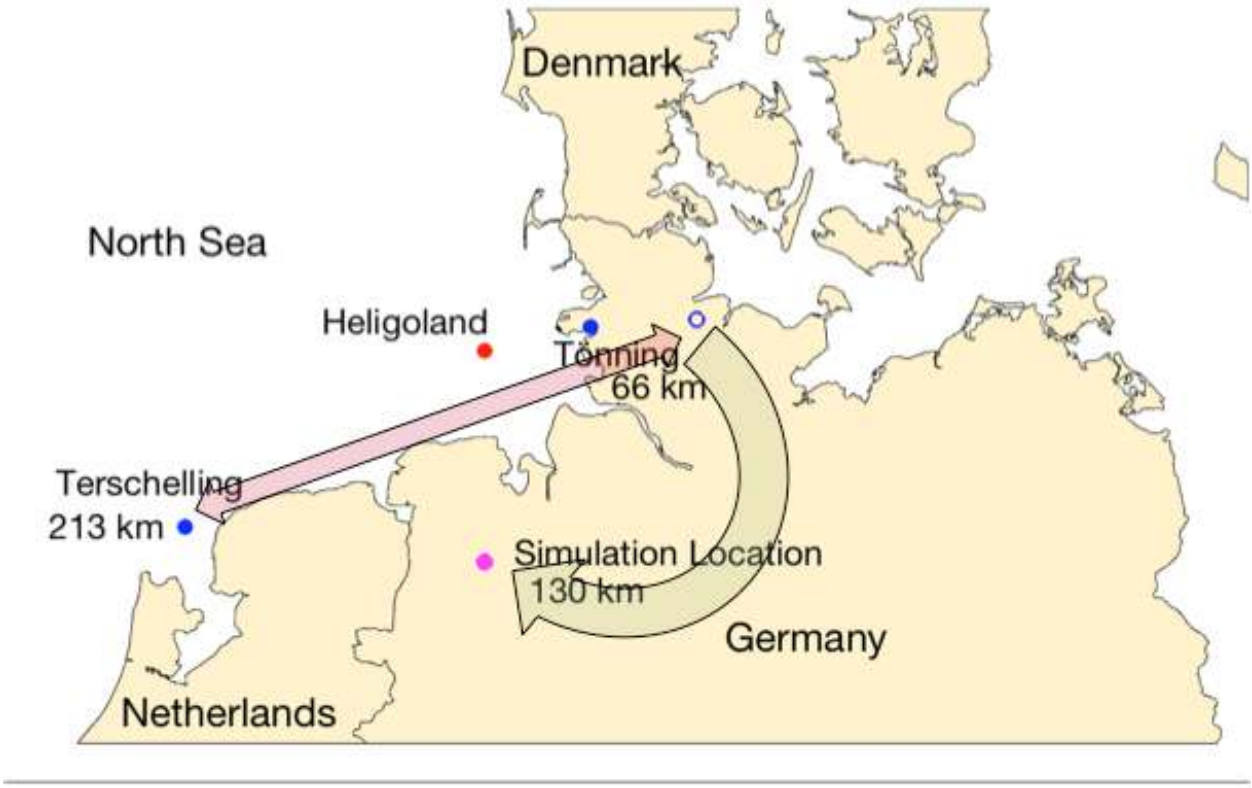

Figure 10: Sites used for the position simulation.

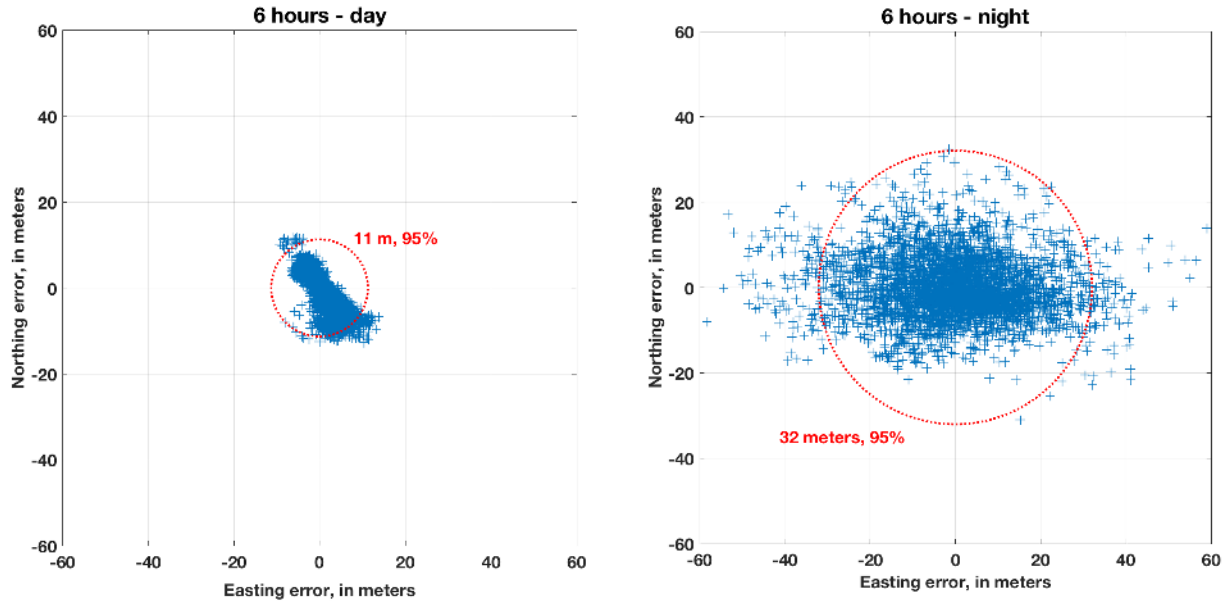

Figure 11: Performance of the simulated positioning experiment. The red circle is the 95% error radius.

R-MODE INTERFERENCE ON LEGACY USERS

Another issue of concern when testing MF DGNSS R-Mode is its impact on legacy DGNSS users. Specifically, to ensure that R-Mode does not negatively impact legacy users, we need to identify how the added CW signals, both in-band and out-of-band, impact the MSK demodulation.

The signal specification for DGNSS [12, 14] does not provide much in the way of noise/interference regulation other than the table of Protection Ratios (reproduced below as Table 2) defining a receiver's response to interfering signals both at the desired channel (0 kHz frequency separation) and for adjacent channels. (We note that the standards only look to channels offsets up to ±2 kHz based on a receiver front-end bandwidth of 4 kHz). Specifically, the table states how large an interferer could be without resulting in any word errors. Conceptually, this table could be applied to our proposed R-Mode method of adding CW signals into the band for ranging by treating them as interfering radiobeacon signals (A1A).

Table 2: Published protection ratios (from [10]).

Frequency separation between wanted and interfering signal (kHz)	Protection ratio (dB)	
Wanted:	Differential (G1D)	Differential (G1D)
Interfering:	Radio beacon (A1A)	Differential (G1D)
0	15	15
0.5	–25	–22
1.0	–45	–36
1.5	–50	–42
2.0	–55	–47

Based on the information from the standards above, 99% of the MSK power is contained within 1.17*R Hz, where R is the MSK bit rate (see Figure 12 for an illustration of this power spectrum, with R=200 bps). In this figure it is clear that most of the area under the MSK curve is contained within the yellow 99% bounds (it is less obvious visually when plotted on a dB scale which magnifies the small values).

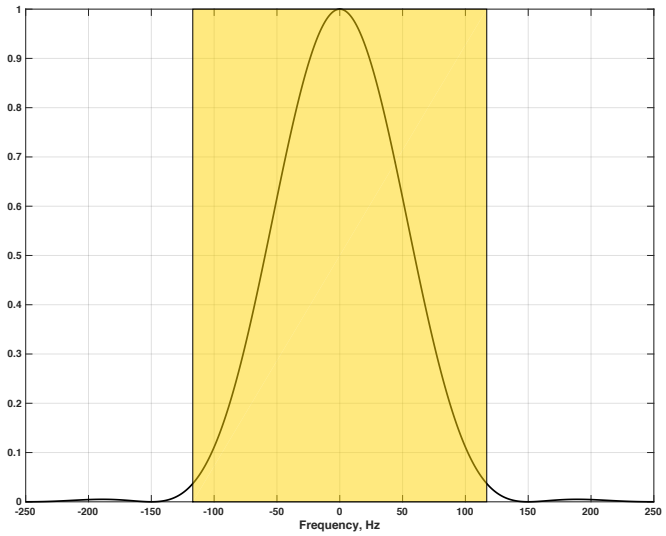

Figure 12: 200 bps MSK signal power envelope with 99% containment BW in yellow.

Figure 13 shows the same 200 bps MSK signal plotted on a dB scale along with the protection limits from Table 2. If we assume that the desired signal is normalized to 0 dB power, then the yellow box shows the power level of 0 dB as well as the 99% bandwidth. The black line shows the power spectral density (PSD) of the desired MSK signal (for 0 dB power, the peak

of the PSD is at -18 dB at the center frequency. The protection limits are based on the signal power (which are based on the 99% bandwidth even though the table pins them at just the center frequency), so they are shown as horizontal lines which cover the 500 Hz bandwidth of the channel. Both sets of protection limits are shown; those for G1D in dotted lines, and those for A1A in dashed lines. The PSDs of the interfering signals that correspond to power levels at the protection limits are shown in red for the in-band and blue for the out-of-band (in decreasing line thickness the farther from the band). In each band, the MSK PSDs are shown with dotted lines and the companion R-mode CWs with dashed lines (corresponding to the line type of the green protection limit lines).

For the R-Mode CW signals, the power is equal to $0.5A^2$, where A is the CW amplitude. Since the CW amplitudes are set at half the amplitude of the MSK signal, the power in each CW signal is at -6 dB relative to the MSK power. The CW power levels are indicated in Figure 13 by the vertical lines at the CW frequencies, the height of the line indicating the CW power.

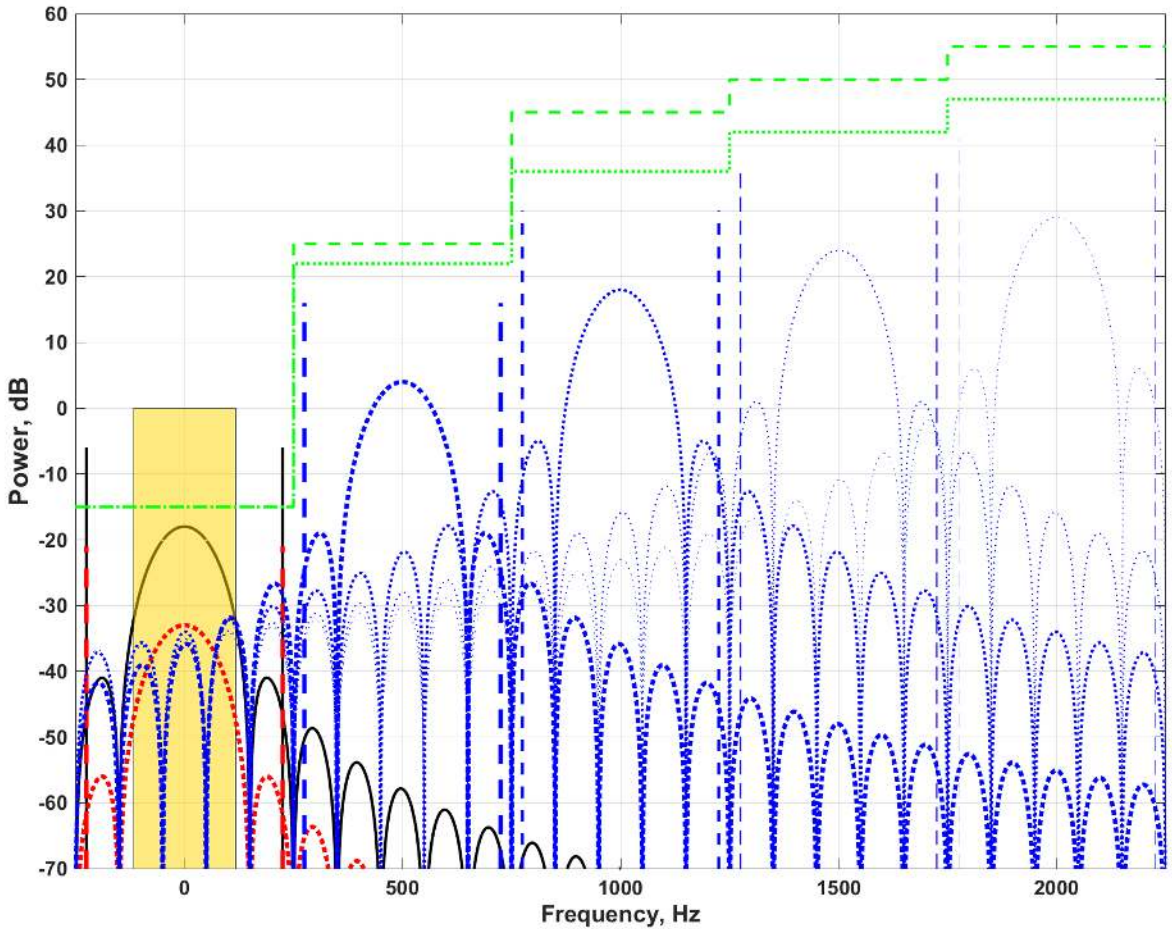

Figure 13: MSK PSDs and CW power plotted in dBs: black = desired, red = in-band interferer, blue = out-of-band interferers. MSK in dotted lines, CW signals in dashed lines. Green horizontal lines indicate protection levels (G1D in dotted lines and A1A in dashed lines). All signals plotted at power of the protection level, relative to a 0 dB desired signal. MSK power measured within the 99% BW as indicated by the yellow box.

To consider the impact of a MF DGNSS R-Mode transmission on a legacy user we can consider two cases separately: the impact of the MSK component and the impact of the two CW signals. The analysis to follow is summarized from a report by some of the authors for The General Lighthouse Authorities of the UK and Ireland [15].

MSK through an MSK receiver

Pasupathy [4] provides a clear introduction to MSK communications. Given a bit interval T, carrier frequency, f_c, and a binary data stream with values of ± 1, then the waveform is

$$s_{MSK}(t) = \cos\left(2\pi f_c t \pm \frac{\pi t}{2T}\right)$$

i.e. a unit magnitude sinusoid. For transmission this signal is scaled to amplitude A.

$$s_{MSK}(t) = A\cos\left(2\pi f_c t \pm \frac{\pi t}{2T}\right)$$

The channel then attenuates the signal resulting in a smaller amplitude for the received MSK; for simplicity we assume that this is accommodated within the value *A*.

Pasupathy also shows that an MSK receiver could be implemented by two parallel, but offset coherent demodulation channels, each with a sinusoidal matched filter response of duration 2T seconds (see Figure 14). In this figure the multiplications are by the functions

$$x(t) = \cos\frac{\pi t}{2T}\cos 2\pi f_c t \qquad \text{and} \qquad y(t) = \sin\frac{\pi t}{2T}\sin 2\pi f_c t$$

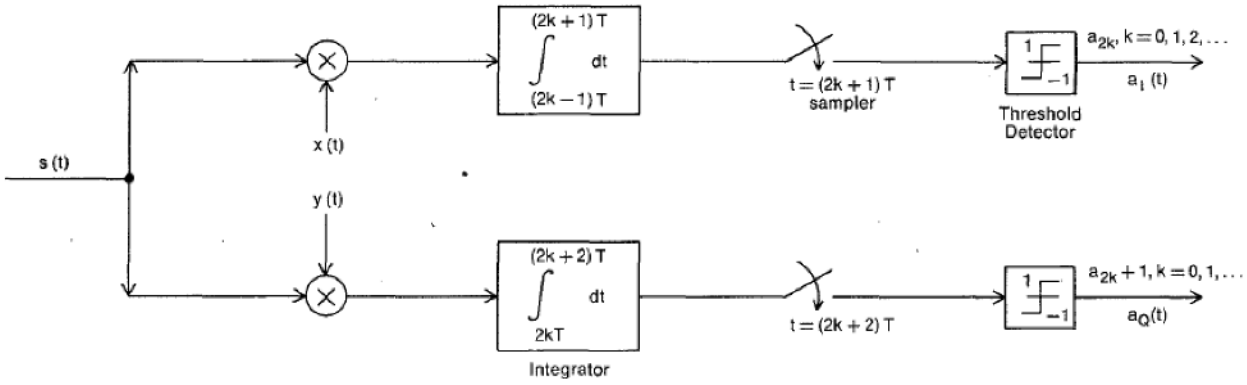

Figure 14: A simple MSK receiver structure (Figure 8 from Pasupathy [4]).

Define Z_{2k} and Z_{2k+1} as the outputs of the samplers in the two receiver paths. Assuming no noise at the receiver and recognizing that the integrator is effectively a low pass filter (and after some simplifications), the first output is well approximated by

$$Z_{2k} \approx \frac{A}{2}\, b_{2k} \int_{(2k-1)T}^{(2k+1)T} \left(1 + \cos\frac{\pi t}{T}\right) dt = \; b_{2k} AT = \pm\frac{1}{2}AT$$

i.e. proportional to the transmitted even bit b_{2k}. Following a similar argument, the bottom channel's output is proportional to the odd bit

$$Z_{2k+1} = \; b_{2k+1}\frac{1}{2}AT = \pm\frac{1}{2}AT$$

and the simple threshold operators at the right of the receiver figure yield the bit stream. If noise and other interference are present, we can model the top sampler's output as

$$Z_{2k} = b_{2k}\frac{1}{2}AT + \; n_{2k} + \; i_{2k}$$

in which n_{2k} and i_{2k} represent the receiver's response to the noise and interference, respectively (recall that the receiver is linear, so these components are additive). The bits are still perfectly decodable as long as $|n_{2k} + i_{2k}| < AT$; a combined

noise and interference component larger than AT in the wrong direction would cause a bit error. As we will refer to this again below, for 200 bps DGNSS this limit is $AT/2 = 0.0025A = 2.5A\times10^{-3}$.

Interfering In-Band MSK

The analysis above can be used directly to describe the response of the MSK receiver to an undesired, interfering MSK signal in the same channel. Imagine that this signal has amplitude A_i, so

$$s_{int-MSK}(t) = A_i \cos\left(2\pi f_c(t-\tau) \pm \frac{\pi(t-\tau)}{2T}\right)$$

in which we include a time shift, τ, recognizing that the interfering signal need not be synchronized with the MSK signal of interest (and, hence, the receiver's matched filter). We wish to compute the response of the top receiver path (multiplier, integrator, and sampler) to it

$$Z_{2k,int-MSK} \equiv \int_{(2k-1)T}^{(2k+1)T} s_{int-MSK}(t)\, x(t)\, dt$$

to see how much effect the interfering signal has on the bit decision. Recall that the definition of a matched filter is that it is the linear system that maximizes the signal to noise ratio at the output of the sampler for the signal of interest. (Equivalently, it is the linear system that maximizes the output of the sample while keeping the noise variance fixed.) Conversely, the maximum output at the sampler for this given filter occurs for a signal proportional to the signal of interest; hence,

$$\max_{\tau} Z_{2k,int-MSK} = Z_{2k,int-MSK}\big|_{\tau=0} = A_i T$$

Further, the response is maximized when the interfering MSK is at the same rate (bps) as the desired one. Table 2 specifies that an in-band interferer must be 15 dB below the desired MSK; i.e. $A_i = A\times10^{-15/20} = 0.1778\,A$ so that the maximum response at the detector is $A_i T = 8.89A\times10^{-4}$, well below the response to the desired MSK ($2.5A\times10^{-3}$), a factor of 2.8 larger in fact, leaving some headroom for noise and other interference.

CW through an MSK receiver

Consider the response of this same MSK receiver to a single CW signal. Specifically, imagine the interfering input to be

$$s_{CW}(t) = B\cos(2\pi f t + \phi)$$

for arbitrary amplitude B, frequency f, and phase offset ϕ. The output of the top receiver path in Figure 14 can be shown to be well approximated by

$$Z_{2k,CW} \approx \frac{B}{2}\cos(4k\pi f_o T + k\pi + \phi)\left(\frac{\sin\left(2\pi\left(f_o + \frac{1}{4T}\right)T + \phi\right)}{2\pi\left(f_o + \frac{1}{4T}\right)} + \frac{\sin\left(2\pi\left(f_o - \frac{1}{4T}\right)T + \phi\right)}{2\pi\left(f_o - \frac{1}{4T}\right)}\right)$$

While a useful expression, being a function of the frequency offset of the CW, f_o, and the bit interval, T, this expression also contains the nuisance variables k and ϕ. From the perspective of evaluating the impact of CW interference on the legacy output, and recognizing that the receiver processing is linear (meaning that the response due to a sum of inputs is equal to the sum of responses), we are really interested in the maximum absolute value of this response to be sure that it does not cause the MSK receiver to make a bit error (i.e. change the sign of the decision variable). Since the leading cosine term is bounded between -1 and $+1$ for all values of f_o and T, we have

$$\max_k\left|Z_{2k,CW}(f_o,T,k,\phi)\right| \le \frac{B}{2}\left|\frac{\sin\left(2\pi\left(f_o + \frac{1}{4T}\right)T + \phi\right)}{2\pi\left(f_o + \frac{1}{4T}\right)} + \frac{\sin\left(2\pi\left(f_o - \frac{1}{4T}\right)T + \phi\right)}{2\pi\left(f_o - \frac{1}{4T}\right)}\right|$$

which removes the dependence on the interval k. To deal with ϕ we evaluate this result for multiple values of ϕ on the range 0 to 2π. Note that an analysis of the bottom path of the receiver yields the same upper bound on the magnitude of its response to the interfering CW.

Assuming that $B = 1$ and $T = 1/200$ (200 bps MSK), Figure 15 shows the magnitude of the receiver's upper path's (the lower path is equivalent) response on a logarithmic scale versus f_o for multiple values of ϕ. Since the CW phase is unknown, we use the worst case for choice for each offset frequency; the upper envelope of the dark region. The peaks at ± 50 Hz are expected in that these are the frequency offsets that the MSK receiver is looking for when $T = 1/200$ (200 bps MSK). Except for narrow bands about ± 50 Hz, the MSK receiver is quite insensitive to CW interference.

As an example for interpreting this result, consider the R-Mode CW signals at $f_o = 225$ Hz with an amplitude $B = 0.5A$. Using the computation results in Figure 15, the output due to this single CW is $8.27\ A \times 10^{-5}$ (the maximum filter response from Figure 4 of 1.65×10^{-4} times the CW amplitude $0.5A$). Even with two such CWs, the worst-case impact at the bit detector is 3.30×10^{-4}, well below the value due to the desired bit ($2.5A \times 10^{-3}$). The computation for other CW frequencies is done in a like manner.

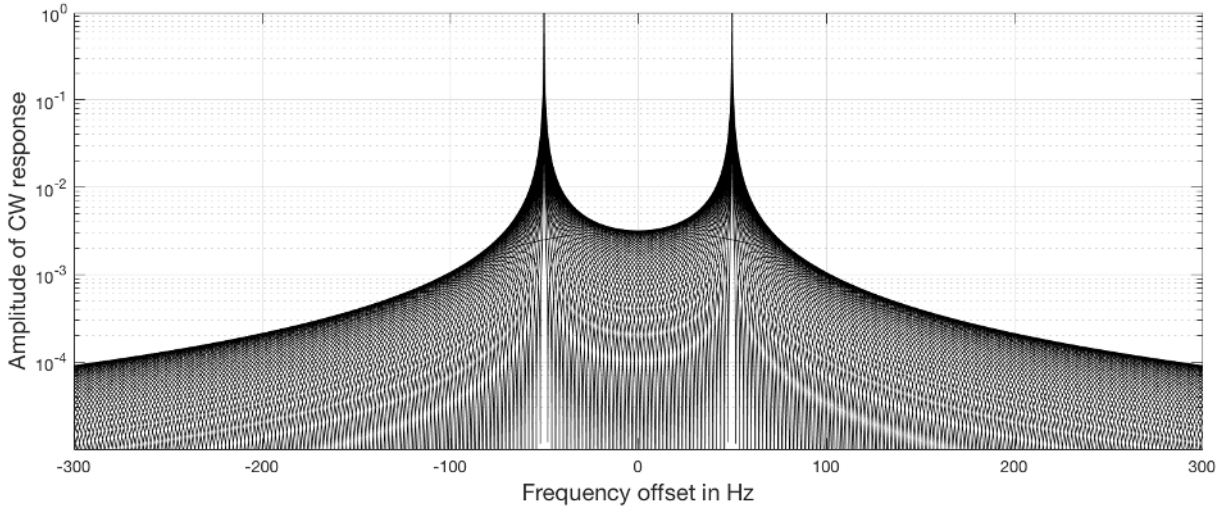

Figure 15: Magnitude response of the receiver to a unit amplitude CW signal.

Impact of a Single R-Mode Transmission

The purpose of the Section has been to consider the response of a legacy MF DGNSS receiver to MF R-Mode transmissions from a single transmitter (we commented at the beginning of this Section that experimentation to date shows no evidence of an impact). To aid in the analysis, recall that since the receiver channels are linear systems, we can add the effects of any interference.

We consider several cases of potential interference to the desired MSK signal: an R-Mode (CW) signal that is being transmitted with the MSK (same transmitter), and an R-Mode (CW) signal that is being transmitted by a different station that is either in the same band or one of four adjacent bands (on either side). In each case, let A represent the received amplitude of the desired MSK signal. Further, assuming 200 bps MSK, our performance benchmark is how the R-Mode response (at the bit decision point) compares to the amplitude of the receiver's response to the desired signal ($2.5A \times 10^{-3}$). The results are presented in Table 3 with some highlights here:

- R-Mode being transmitted along with MSK: The worst-case interference to the two CWs at ± 225 Hz is $1.65A \times 10^{-4}$, only 6% of the error margin of $2.5A \times 10^{-3}$, small when compared to the interference level of a co-channel MSK transmission (36% of the error margin).
- Interfering R-Mode in the same channel: The significant protection ratio for this co-channel interference (15 dB) makes the worst-case interference to the two CWs at ± 225 Hz very small, $2.94\ A \times 10^{-5}$, or 1.2% of the error margin.
- Interfering R-Mode in any of the four adjacent channels, up or down in frequency: In each of these cases the contribution of the two CWs is manageable, at most $7.81\ A \times 10^{-4}$ (found in the first adjacent band) or 32% of the error margin, still less than the impact of interfering co-channel MSK.

In conclusion, as observed anecdotally, a single R-Mode transmission has negligible impact on legacy MSK performance.

Table 3: R-Mode impacts at the linear receiver – in-band signals.

Case	Signal	Value
Desired signal is R-Mode	Amplitude of each R-Mode CW signal, $B = A/2$	$0.5\ A$
	Maximum receiver output due to the two R-Mode CW signals on the desired station ($f_o = \pm 225$ Hz)	$1.65A \times 10^{-4}$
R-Mode interference in the same channel	Amplitude of the interfering, in-band MSK signal (15 dB protection ratio) $A_i = A \times 10^{-PR/20}$	$0.178\ A$
	Maximum receiver output due to the in-band MSK interferer, $R = A_i T$	$8.89\ A \times 10^{-4}$
	Maximum receiver output due to the two R-Mode CW signals on the interfering in-band MSK (± 225 Hz), at amplitude $B_i = A_i/2$	$2.94\ A \times 10^{-5}$
R-Mode interference in a channel offset by ±500 Hz	Maximum receiver output due to the two R-Mode CW signals in the first adjacent band ($\pm 275, \pm 725$ Hz), -22 dB protection ratio	$7.81\ A \times 10^{-4}$
R-Mode interference in a channel offset by ±1000 Hz	Maximum receiver output due to the two R-Mode CW signals in the second adjacent band ($\pm 775, \pm 1225$ Hz), -36 dB protection ratio	$5.87\ A \times 10^{-4}$
R-Mode interference in a channel offset by ±1500 Hz	Maximum receiver output due to the two R-Mode CW signals in the third adjacent band ($\pm 1275, \pm 1725$ Hz), -42 dB protection ratio	$4.77\ A \times 10^{-4}$
R-Mode interference in a channel offset by ±2000 Hz	Maximum receiver output due to the two R-Mode CW in the fourth adjacent band ($\pm 1775, \pm 2225$ Hz), -47 dB protection ratio	$4.63\ A \times 10^{-4}$

CONCLUSIONS

Investigations to date bear out the predictions of the Feasibility Study [6] and suggest that the phase of the CW signals can be tracked well enough to yield good positioning performance out to 200 km. During the day the performance of all three ranges is better than 10 m, while at night, due to the influence of skywave, the performance decreases, but is still around 20m or less (the Feasibility Study assumed a night time performance an order of magnitude worse than the daytime performance). The positioning performance predicted by our data appears to be on the order of 11m 2DRMS during the day and 32m 2DRMS at might. Whether the achievable performance level is acceptable or not for a back-up system needs to be determined by the Competent Authority.

The propagation speed of ground wave signals such as the proposed R-Mode CW vary during the course of the day and season; this temporal ASF effect is visible in the current data and has been previously noticed with Loran signals at 100 kHz. Such temporal effects can be dealt with by using reference stations to track the variations, transmitting "corrections" on the MSK signal or some other augmentation channel.

An examination of a standard MSK receiver suggests that the CW R-Mode signal will not compromise the performance of legacy DGNSS receivers. The addition of CW components to the legacy MSK transmission (self interference) increases the interference by only 3% of the error margin. The addition of CW components to interfering signals adds less than 1% for an in band, and at most 16% for an adjacent band signal, assuming the signals are at the maximum power allowed by the protection ratio table. In comparison, an in-band interfering MSK signal at the allowed power, results in an interference level of 18% of the error.

If additional protection for legacy receivers is desired, there are four options:

1. Reduce the amplitude of the CW signals.
2. Reduce the spacing of the CW frequencies.
3. Dropping one of the CW signals.
4. Reduce the MSK bit rate.

There is, of course, other consequences of doing any of these, which need to be considered.

FUTURE WORK

In order to develop and test positioning receivers, additional R-Mode transmitters are needed; two for ranging mode and three for pseudorange mode. The WSV has already set up a 2nd transmitter (at Zeven), which will enable experiments with ranging modes. Hopefully a third will soon follow to allow testing of pseudorange mode. In addition, works needs to be done developing and testing cycle ambiguity resolution procedures for the CW phase as to date, this has been assumed to be fixed. Additionally, work needs to be done to estimate the impact of the ASF temporal variations in order to determine the required number of reference stations. We note that the density of DGNSS transmitters in ITU Region I suggests co-locating the reference stations with the transmitters. It also appears likely that the spatial ASF variation can be ignored due to the short ranges to the transmitters.

The R-Mode interference study needs to be completed to examine the case of multiple R-mode interferers, and how that compares to the existing scenarios of multiple MSK interferers.

REFERENCES

[1] J. Raquet. (2006, August) Navigation Using Signals of Opportunity. *GPS World Discussion Forums*.

[2] G. W. Johnson and P. F. Swaszek, "Feasibility Study of R-Mode using MF DGPS Transmissions," German Federal Waterways and Shipping Administration, Milestone 2 Report, 11 March 2014.

[3] G. Johnson, P. Swaszek, J. Alberding, M. Hoppe, and J.-H. Oltmann, "The Feasibility of R-Mode to Meet Resilient PNT Requirements for e-Navigation," in *ION GNSS Conference*, Tampa, FL, 2014.

[4] S. Pasupathy, "Minimum Shift Keying: A Spectrally Efficient Modulation," *IEEE Communications Magazine,* vol. 17, pp. 14-22, 1979.

[5] J. F. Kasper and C. E. Hutchinson, "The Omega navigation system--An overview," *Communications Society Magazine, IEEE,* vol. 16, pp. 23-35, 1978.

[6] G. W. Johnson and P. F. Swaszek, "Feasibility Study of R-Mode combining MF DGNSS, AIS, and eLoran Transmissions," German Federal Waterways and Shipping Administration, Final Report, 25 September 2014.

[7] G. Frenkel and D. Gan, "Ambiguity Resolution in Systems Using Omega for Position Location," *IEEE Transactions on Communications,* vol. 22, pp. 305-312, 1974.

[8] N. DeMinco, "Medium Frequency Propagation Prediction Techniques and Antenna Modeling for Intelligent Transportation Systems (ITS) Broadcast Applications," U.S. Dept. of Commerce NTIA Report 99-368, August 1999.

[9] N. DeMinco, "Propagation Prediction Techniques and Antenna Modeling (150 to 1705 kHz) for Intelligent Transportation Systems (ITS) Broadcast Applications," *IEEE Antennas and Propagation Magazine,* vol. 42, p. 26, August 2000.

[10] G. W. Johnson, P. F. Swaszek, R. Hartnett, R. Shalaev, C. Oates, D. Lown*, et al*., "A Procedure for Creating Optimal ASF Grids for Harbor Entrance & Approach," presented at the ION GNSS 2006, Fort Worth, TX, 2006.

[11] *ITU-R Handbook on the Ionosphere and its Effects on Radiowave Propagation*. Geneva: ITU-R, 1998.

[12] "Broadcast Standard for the USCG DGPS Navigation Service," U.S. Coast Guard, Washington, DC COMDTINST M16577.1, April 1993.

[13] D. C. Poppe, "Coverage and Performance Prediction of DGPS Systems Employing Radiobeacon Transmissions," PhD. Dissertation, University of Wales, Bangor, UK, 1995.

[14] "Maritime Navigation and Radiocommunication Equipment and Systems - Global Navigation Satellite Systems (GNSS) - Part 4: Shipborne DGPS and DGLONASS Maritime Radio Beacon Receiver Equipment - Performance Requirements, Methods of testing and Required Test Results," International Electrotechnical Commission, International Standard IEC 61108-4, 2004.

[15] G. W. Johnson and P. F. Swaszek, "R-Mode Noise Investigation Study," General Lighthouse Authorities of the UK and Ireland, Harwich, UK, Final ReportFebruary 2017.

[16] D. Rife and R. R. Boorstyn, "Single tone parameter estimation from discrete-time observations," *Information Theory, IEEE Transactions on,* vol. 20, pp. 591-598, 1974.

[17] D. C. Rife and R. R. Boorstyn, "Multiple Tone Parameter Estimation from Discrete-Time Observations," *Bell Systems Technical Journal,* pp. 1389 - 1410, November 1976.

[18] S. M. Kay, *Fundamentals of Statistical Signal Processing, Volume I: Estimation Theory*: Prentice Hall, 1993.

ACKNOWLEDGEMENTS

This work has been funded by the German Federal Waterways Administration and the General Lighthouse Authorities of the UK and Ireland.

APPENDIX A – RANGE ESTIMATE FROM THE CW

For simplicity, consider just the CW portion of the broadcast and write the received signal as the sum of the transmitted CW (frequency f_m) and noise

$$r(t) = A\cos 2\pi f_m(t-\tau) + w(t)$$

In this expression A is the received amplitude and τ accounts for the propagation delay (nominally equal to d/c, d being the range from the transmitter and c the speed of light, plus factors pertaining to speed of propagation and channel effects); $\mathrm{w(t)}$ is the noise, assumed to have variance σ^2. Converting to phase angle, this received signal is

$$r(t) = A\cos(2\pi f_m t + \theta) + w(t)$$

in which $\theta = 2\pi f_m \tau$. In other words, the propagation delay is manifested as a phase shift and, because of the periodic nature of the sine function, the range can only be estimated with an ambiguity dependent upon the wavelength of the sinusoid (approximately 1 km for the MF DGNSS band).

Estimating the phase in such a situation is well understood; relevant references include Rife [16, 17] and Kay [18]. Sampling every $\mathrm{T_s}$ seconds we have the data sequence

$$r[n] = A\cos(2\pi f_m n T_s + \theta) + w[n]$$

for $\mathrm{n} = 0, 1, \ldots \mathrm{N}-1$ and are interested in estimators $\hat{\theta}$ for the unknown phase. A lower bound to the variance of any unbiased estimate is the Cramer-Rao Bound (CRB). For the sampled version of this problem this is

$$\mathrm{Var}(\hat{\theta}) \geq \frac{2\sigma^2}{A^2 N}$$

Noting that the signal to noise ratio, SNR, for this signal is $\mathrm{SNR} = \frac{A^2}{2\sigma^2}$, then the CRB is $\mathrm{Var}(\hat{\theta}) \geq \frac{1}{N\ \mathrm{SNR}}$ and the variance decreases as both N and the SNR increase (as would be expected).

The maximum likelihood estimate (MLE) of θ involves projecting the received signal onto both the sine and cosine functions of the same frequency and using the arc-tangent function (on the full 0 to 2π range) to recover θ

$$\hat{\theta}_{MLE} = -\,\mathrm{atan}\left(\frac{\sum_{n=0}^{N-1} x[n]\sin 2\pi f_m n T_s}{\sum_{n=0}^{N-1} x[n]\cos 2\pi f_m n T_s}\right)$$

We note:

This estimator is asymptotically efficient in that as N goes to infinity then the distribution of the estimate converges to a Gaussian density with mean equal to the true phase and variance equal to the CRB.

The MLE of the range (without solution of the ambiguity) is this phase estimate transformed to distance using the wavelength of the sinusoid

$$\hat{r}_{MLE} = -\frac{c}{2\pi f_m}\,\mathrm{atan}\left(\frac{\sum_{n=0}^{N-1} x[n]\sin 2\pi f_m n T_s}{\sum_{n=0}^{N-1} x[n]\cos 2\pi f_m n T_s}\right)$$

For two CW signals in white noise the joint MLE is just the pair of separate MLEs.

APPENDIX B – RESPONSE OF A MSK DEMODULATOR TO CW INTERFERENCE

Pasupathy [4] provides a clear introduction to MSK communications. First, he shows that the MSK signal can be written as a form of offset (by T seconds) quadrature modulation

$$s_{MSK}(t) = a_I(t)\cos\frac{\pi t}{2T}\cos 2\pi f_c t + a_Q(t)\sin\frac{\pi t}{2T}\sin 2\pi f_c t$$

in which $a_I(t)$ and $a_Q(t)$ are the in-phase (even) and quadrature (odd) bits

$$\begin{aligned} a_I(t) &= b_{2k} \qquad (2k-1)T < t < (2k+1)T \\ a_Q(t) &= b_{2k+1} \qquad 2kT < t < (2k+2)T \end{aligned}$$

T is the bit interval, and f_c is the carrier frequency. Note that since the bits are either $+1$ or -1 then the waveform is

$$s_{MSK}(t) = \pm\cos\frac{\pi t}{2T}\cos 2\pi f_c t \pm \sin\frac{\pi t}{2T}\sin 2\pi f_c t$$

or, by trigonometric identity,

$$s_{MSK}(t) = \pm\cos\left(2\pi f_c t \pm \frac{\pi t}{2T}\right)$$

i.e. a unit magnitude sinusoid. Further, with this form it is obvious that the sinusoid either advances or retards by $\frac{\pi}{2}$ radians (90 degrees) every T seconds.

Pasupathy also shows that an MSK receiver could be implemented by two parallel, but offset coherent demodulation channels, each with a sinusoidal matched filter response of duration 2T seconds (see Figure 13). In this figure

$$x(t) = \cos\frac{\pi t}{2T}\cos 2\pi f_c t \qquad \text{and} \qquad y(t) = \sin\frac{\pi t}{2T}\sin 2\pi f_c t$$

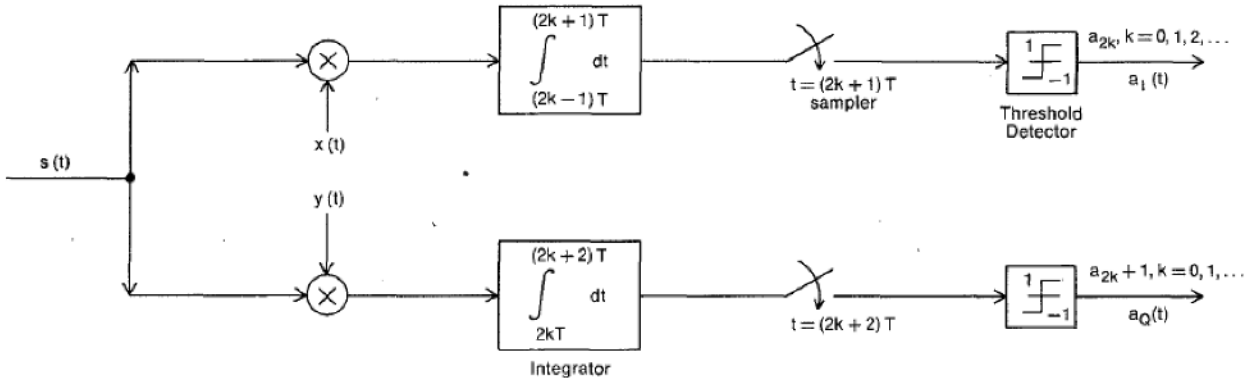

Figure 13: A simple MSK receiver structure (Figure 8 from Pasupathy [4]).

Assuming no noise, the output of the top multiplier during $(2k-1)T < t < 2kT$ is

$$z(t) = s_{MSK}(t)\,x(t) = b_{2k}\cos^2\frac{\pi t}{2T}\cos^2 2\pi f_c t + b_{2k-1}\sin\frac{\pi t}{2T}\cos\frac{\pi t}{2T}\sin 2\pi f_c t\ \cos 2\pi f_c t$$

while during $kT < t < (2k+1)T$ it is

$$z(t) = s_{MSK}(t)\,x(t) = b_{2k}\cos^2\frac{\pi t}{2T}\cos^2 2\pi f_c t + b_{2k+1}\sin\frac{\pi t}{2T}\cos\frac{\pi t}{2T}\sin 2\pi f_c t\ \cos 2\pi f_c t$$

Employing trigonometric identities these are for $(2k-1)T < t < 2kT$

$$z(t) = b_{2k}\cos^2\frac{\pi t}{2T} + b_{2k}\cos^2\frac{\pi t}{2T}\cos 4\pi f_c t + b_{2k-1}\sin\frac{\pi t}{T}\sin 4\pi f_c t$$

while during $kT < t < (2k+1)T$

$$z(t) = b_{2k}\cos^2\frac{\pi t}{2T} + b_{2k}\cos^2\frac{\pi t}{2T}\cos 4\pi f_c t + b_{2k+1}\sin\frac{\pi t}{T}\sin 4\pi f_c t$$

The second and third terms in both of these expressions are at frequencies near $2f_c$; hence, are filtered out by the integrator (which operates, essentially, as a low pass filter) and the low pass portions for both periods are the same

$$z(t)_{LP} = b_{2k}\cos^2\frac{\pi t}{2T} = b_{2k}\left(1+\cos\frac{\pi t}{T}\right)$$

Integrating, the sampler output:

$$\int_{(2k-1)T}^{(2k+1)T} z(t)\,dt \approx b_{2k}\int_{(2k-1)T}^{(2k+1)T}\left(1+\cos\frac{\pi t}{T}\right)dt = b_{2k}2T = \pm 2T$$

is proportional to the transmitted even bit. Following a similar argument, the bottom channel's outputs are proportional to the odd bits and the simple threshold operators at the right of the receiver figure yield the bit stream. If noise is present we can model the sampler's output as

$$b_{2k}2T + n_{2k}$$

in which n_{2k} is a noise variable. The bits are still perfectly decodable as long as $|n_{2k}| < 2T$; a noise component larger than T in the wrong direction would cause a bit error.

To examine the effects of R-Mode CW interference on the MSK receiver, let's repeat this analysis for a CW signal. Specifically, imagine the interfering input to be

$$s_{CW}(t) = A\cos(2\pi f t + \phi)$$

for some arbitrary amplitude A and phase offset ϕ. The output of the top multiplier during time interval $(2k-1)T < t < (2k+1)T$ is

$$\begin{aligned} z_{CW}(t) = s_{CW}(t)\,x(t) &= A\cos(2\pi f t+\phi)\cos\frac{\pi t}{2T}\cos 2\pi f_c t \\ &= \frac{A}{2}\cos\frac{\pi t}{2T}\cos(2\pi(f-f_c)t+\phi) + \frac{A}{2}\cos\frac{\pi t}{2T}\cos(2\pi(f+f_c)t+\phi) \end{aligned}$$

For interfering CW with frequency near f_c then the second term is near frequency $2f_c$ and is removed by the integrator; the low pass portion is

$$z_{CW}(t)_{LP} = \frac{A}{2}\cos\frac{\pi t}{2T}\cos(2\pi f_o t+\phi) = \frac{A}{4}\cos\left(2\pi\left(f_o+\frac{1}{4T}\right)t+\phi\right) + \frac{A}{4}\cos\left(2\pi\left(f_o-\frac{1}{4T}\right)t+\phi\right)$$

in which we define the offset frequency $f_o = f - f_c$. Integrating, the sampler output is

$$\begin{aligned} &\int_{(2k-1)T}^{(2k+1)T} z_{CW}(t)\,dt \\ &\qquad \approx \frac{A}{4}\frac{\sin\left(2\pi\left(f_o+\frac{1}{4T}\right)(2k+1)T+\phi\right) - \sin\left(2\pi\left(f_o+\frac{1}{4T}\right)(2k-1)T+\phi\right)}{2\pi\left(f_o+\frac{1}{4T}\right)} \\ &\qquad + \frac{A}{4}\frac{\sin\left(2\pi\left(f_o-\frac{1}{4T}\right)(2k+1)T+\phi\right) - \sin\left(2\pi\left(f_o-\frac{1}{4T}\right)(2k-1)T+\phi\right)}{2\pi\left(f_o-\frac{1}{4T}\right)} \end{aligned}$$

This result appears in Figure 12 for multiple values of ϕ.